Environmental Pollution 337 (2023) 122561

Contents lists available at ScienceDirect

Environmental Pollution

journal homepage: www.elsevier.com/locate/envpol

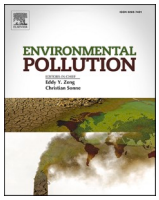

Nepalese indoor cookstove smoke extracts alter human airway epithelial gene expression, DNA methylation and hydroxymethylation☆

Poojitha Rajasekar [a,b,c], Robert J. Hall [a,b,c], K.C. Binaya [a,d], Parth S. Mahapatra [d], Siva P. Puppala [d], Dhruma Thakker [a,b,c], Julia L. MacIsaac [e], David Lin [e], Michael Kobor [e], Charlotte E. Bolton [a,b], Ian Sayers [a,b,c], Ian P. Hall [a,b,c], Rachel L. Clifford [a,b,c,*]

[a] Centre for Respiratory Research, Translational Medical Sciences, School of Medicine, University of Nottingham, UK
[b] Nottingham NIHR Biomedical Research Centre, Nottingham, UK
[c] Biodiscovery Institute, University Park, University of Nottingham, UK
[d] Water and Air Theme, Atmosphere Initiative, International Centre for Integrated Mountain Development, Kathmandu, Nepal
[e] BC Children's Hospital Research Institute, Department of Medical Genetics, University of British Columbia, Vancouver, British Columbia, Canada

ARTICLE INFO

Keywords:
Cookstoves
Airway epithelium
DNA methylation
DNA hydroxymethylation
Gene expression
Nepal

ABSTRACT

Household air pollution caused by inefficient cooking practices causes 4 million deaths a year worldwide. In Nepal, 86% of the rural population use solid fuels for cooking. Over 25% of premature deaths associated with air pollution are respiratory in nature. Here we aimed to identify molecular signatures of different cookstove and fuel type exposures in human airway epithelial cells, to understand the mechanisms mediating cook stove smoke induced lung disease. Primary human airway epithelial cells in submerged culture were exposed to traditional cook stove (TCS), improved cook stove (ICS) and liquefied petroleum gas (LPG) stove smoke extracts. Changes to gene expression, DNA methylation and hydroxymethylation were measured by bulk RNA sequencing and HumanMethylationEPIC BeadChip following oxidative bisulphite conversion, respectively. TCS smoke extract alone reproducibly caused changes in the expression of 52 genes enriched for oxidative stress pathways. TCS, ICS and LPG smoke extract exposures were associated with distinct changes to DNA methylation and hydroxymethylation. A subset of TCS induced genes were associated with differentially methylated and/or hydroxymethylated CpGs sites, and enriched for the ferroptosis pathway and the upstream regulator NFE2L2. DNA methylation and hydroxymethylation changes not associated with a concurrent change in gene expression, were linked to biological processes and molecular pathways important to airway health, including neutrophil function, transforming growth factor beta signalling, GTPase activity, and cell junction organisation. Our data identified differential impacts of TCS, ICS and LPG cook stove smoke on the human airway epithelium transcriptome, DNA methylome and hydroxymethylome and provide further insight into the association between indoor air pollution exposure and chronic lung disease mechanisms.

1. Introduction

2.6 billion people across the world cook using open fires or simple biomass fuelled stoves, and the World Health Organisation attributes approximately 4 million deaths worldwide to illness linked to household air pollution from inefficient cooking practices (Organisation, 2021). The majority of these are in low- and middle-income countries (Organisation, 2021). In 2011 in Nepal 74% of the total population relied on solid fuels for cooking, rising to 86% of the population in rural areas (Paudel et al., 2020). However, usage of liquefied petroleum gas (LPG) and improved cook stoves, which use solid fuels with improved combustions systems and/or chimneys to vent fumes, are increasing.

Over 25% of premature deaths associated with air pollution are respiratory in nature. Adverse respiratory effects of air pollution include decreased pulmonary function, increased infections, acute exacerbations of Chronic Obstructive Pulmonary Disease (COPD), increased

☆ This paper has been recommended for acceptance by Admir Créso Targino.

* Corresponding author. Centre for Respiratory Medicine, Translational Medical Sciences School of Medicine, Faculty of Medicine and Health Sciences, University of Nottingham, C213, Biodiscovery Institute, University Park, Nottingham, NG7 2RD, UK.
E-mail address: R.clifford@nottingham.ac.uk (R.L. Clifford).

https://doi.org/10.1016/j.envpol.2023.122561
Received 4 May 2023; Received in revised form 12 September 2023; Accepted 13 September 2023
Available online 22 September 2023

hospitalisations, increased respiratory mortality and higher prevalence of asthma (Jiang et al., 2016; Raju et al., 2020). Mechanistically, inhaled pollutants acutely damage the airway epithelium (Cao et al., 2020) and alter airway (Jiang et al., 2022; Fujii et al., 2001) and nasal (Montgomery et al., 2020) epithelium inflammatory gene expression. Furthermore, exposure of human lung tissue to smoke extracts derived from traditional cook stoves (TCS), improved cook stove (ICS) and LPG stoves used in Nepal, increases inflammatory cytokine secretion (Kc et al., 2020). Personal exposure to particulate matter with an aerodynamic diameter of <2.5 μm ($PM_{2.5}$) and carbon monoxide is dramatically reduced by transition from TCSs to ICSs/LPG (Kc et al., 2020) however, the underlying molecular mechanisms mediating these cook stove smoke induced changes to the epithelium have not been studied. Comparative analysis of their effects on airway relevant cell types will inform our understanding of airways biology in response to exposure and identify drivers of disease in exposed populations.

DNA methylation is a mechanism whereby environmental exposures can regulate gene expression and potentially leave a "memory" of exposure to impart long term effects. DNA methyltransferases (DNMTs) deposit methyl groups onto cytosine residues to generate DNA 5-methylcytosine (5 mC) while Ten-eleven translocation (TET) methyl cytosine dioxygenases catalyse the oxidation of 5 mC to 5-hydroxymethylcytosine (5 hmC), 5-formylcytosine (5 fC) and 5-carboxycytosine (5 cC) as part of an active demethylation process. 5 hmC is more stable than 5 fC/cC and a regulator of transcription in its own right (Audrey Lejart, 2018). Blood DNA methylation levels are associated with particulate matter concentration (Wang et al., 2020; Chi et al., 2016; Panni et al., 2016), short term human exposure to diesel exhaust (with allergen exposure) alters airway epithelial cell DNA methylation (Clifford, 2017), TET/DNMT expression and global mC and hmC (Clifford, 2017; Li et al., 2021), and *in vitro* exposure to $PM_{2.5}$ from biomass (Hesselbach et al., 2017) and ambient air (Shi et al., 2019) changes DNA methylation and gene expression in immortalised human bronchial epithelial cells.

The aims of the current study were to understand the comparative effects of short-term exposure to traditional, improved and LPG cook stove smoke exposure of primary human airway epithelial cell responses by profiling gene expression, DNA methylation, and DNA hydroxymethylation.

2. Materials and methods

2.1. Sample collection and preparation

Biomass combustion smoke from TCSs, ICSs and LPG stoves and ambient air (AA) in Salambu, Nepal, was channelled through 10 mL media (DMEM, Dulbecco's Modified Eagle's Medium, ThermoFisher Scientific) using an impinger system and vacuum pump at a constant flow rate of 3 L/m throughout a 1 h cooking duration to generate combustion smoke extract (SE). The sample was immediately stored in a temporary field freezer below −10 °C and subsequently stored at −20 °C. Further details are provided in the supplemental material.

2.2. Human bronchial epithelial cells (HBEC) stimulations

HBECs were purchased from Lonza (Wokingham, UK). HBECs were maintained in PneumaCult-Ex Basal Medium (490 mL PneumaCult-Ex Basal Medium plus 10 mL PneumaCult-Ex 50 x Supplement and 500 μL 200X hydrocortisone stock solution) with the addition of 5 mL antibiotic, antimycotic solution containing penicillin, streptomycin and fungizone (PSF). HBECs were cultured (Rayner et al., 2019) and seeded in 6 well plates at 75,000 cells/well in 2 mL media with media changes every 48 h. Upon reaching 90% confluence cells were treated with TCS, ICS, LPG, and ambient air (AA) by adding 200 μL of stock solution to the cells in 1.8 mL media. Cells were left in media with added treatment for 24 h. Exposures were performed as two distinct phases; here termed a discovery and a replication experiment as gene expression data were available for both data sets. Both phases were performed as six independent experiments (2 donors, each on three separate occasions Table S1). DNA methylation (methyl and hydroxymethyl cytosine) data were available for the replication experiment only.

2.3. DNA/RNA isolation

Cell lysates were harvested in 300 μL RLT plus buffer with 3 μL β-mercaptoethanol. Lysates were stored at −80 °C. DNA and RNA were isolated from lysates using the All Prep DNA/RNA Mini Kit as per the manufacturer's instruction (Qiagen).

2.4. RNA sequencing

2.4.1. Library preparation and RNA-sequencing

Library preparation and RNA-sequencing were carried out by Oxford Genomics Centre as previously described (Hall et al., 2021). Briefly, RNA was quantified using RiboGreen (Invitrogen, Glasgow, UK) and the size profile and integrity analysed on the 4200 TapeStation (Agilent). RNA was normalised to 100 ng prior to library preparation. Polyadenylated transcript enrichment and strand specific library preparation was completed using NEBNext Ultra II mRNA kit (NEB, Hitchin, UK) following the manufacturer's instructions. Libraries were amplified on a Tetrad (Bio-Rad, London, UK) using in-house unique dual indexing primers. Individual libraries were normalised (Qubit), and the size profile was analysed on the 4200 TapeStation. Libraries were normalised and pooled together accordingly and diluted to approximately 10 nM for storage. The 10 nM library was denatured and further diluted prior to paired end (75 bp) sequencing (HiSeq4000 platform and HiSeq 3000/4000 PE Cluster Kit and 150 cycle SBS Kit (Illumina, Cambridge, UK)), which generated a raw read count of approximately 30 million reads per sample.

2.4.2. Trimming and alignment of fastq files

Processing of RNA-seq data was performed using the Unix operating system. Quality of fastq files was assessed using fastqc (Andrews). Adaptor and quality trimming of fastq files was performed using Trimmomatic (Bolger et al., 2014). Trimmed reads were aligned to the CRCh37 build using Star producing count files that were used for differential expression analysis (Dobin et al., 2013).

2.4.3. Pre-processing of count files for differential gene expression

Raw counts were converted to counts per million (CPM) and lowly expressed genes across all samples were filtered out of the analysis using the filterByExpr function in EdgeR (Robinson et al., 2010). Normalisation of data was performed using the calcNormFactors in EdgeR using the trimmed mean of M-values (TMM) method.

2.5. DNA methylation array

2.5.1. Bisulphite conversion of DNA and genome wide microarray

One microgram of genomic DNA was used as input material into the TrueMethyl® oxBS module (NuGEN/Tecan). One part of each sample, 500 ng, was oxidized converting hydroxymethylated cytosines (5 hmCs) to formylcytosines (5 fCs). The other 500 ng underwent a mock reaction in the absence of oxidating reagents so that the hydroxymethylated cytosines remained. Both parts were bisulfite-converted as per manufacturer's instructions. In the oxidized part, herein referred to as the oxBS samples, the oxidation-induced 5 fCs were deaminated to uracils so that only the original 5 mC bases remained cytosines. In the conventional bisulfite conversion that underwent the mock reaction, herein referred to as the BS samples, both 5 hmCs and 5 mCs remained cytosines. Thus, hydroxymethylated cytosines (5 hmCs) were indirectly determined as the difference in methylation between the two reactions. 35 pairs and a replicate pair (oxBS and BS samples) were processed using

the Infinium MethylationEPIC BeadChip Kit per manufacturer's instructions (Illumina, San Diego, CA, USA) with one adaptation. To maximize the amount of template used, 7 μL of recovered TrueMethyl® template was used with 1 μL of 0.4 N NaOH, instead of using 4 μL of template and 4 μL of 0.1 N NaOH.

2.5.2. DNA methylation and hydroxymethylation microarray data pre-processing

HumanMethylationEPIC BeadChips were scanned using Illumina HiScan scanner. Raw IDAT files obtained through GenomeStudio software were imported into R Statistical software (version 4.1.0) (R.C.T. and R, 2020) and processed using Bioconductor packages (version 3.13). Pre-processing and quality control were carried out using specific functions in minfi package (version 1.38.0) (Aryee et al., 2014; Fortin et al., 2017). Technical replicates exhibited robust correlation (r = 0.991). Probes were filtered as follows: 87,432 probes with <3 bead count in at least one sample, 65 single nucleotide polymorphism (SNP) probes, 3295 probes with low detection p-value (0.05) in at least 1% of the samples, 10,955 probes with a SNP at targeted CpG binding sites and single base extension sites and 38,417 cross-hybridising probes. Probes annotated to X and Y chromosomes were retained for analysis as both cell donors were female. Identical results were obtained from parallel analysis performed with and without X and Y chromosome probes. 732, 290 probes remained for further analysis. Dasen normalisation (Pidsley et al., 2016) was performed using watermelon package (version 1.36.0) (Pidsley et al., 2013). Correlation of technical replicates improved post normalisation (r = 0.992). The Maximum Likelihood Methylation Levels (MLML) method (Qu et al., 2013) was used to estimate the intensity fractions of methylated and hydroxymethylated cytosine at each CpG site using MLML2R package (version 0.3.3) (Kiihl et al., 2019a). Beta values representing percentage methylation and M values (log transformed beta values) were calculated from methylation (mC) and hydroxymethylation (hmC) fractions obtained from MLML method. M values for both mC and hmC were subject to batch effect correction based on array chip ID using comBat function in SVA package (version 3.40.0) (Leek et al., 2012).

2.6. Gene expression and DNA methylation analysis

2.6.1. Differential gene expression and DNA methylation/hydroxymethylation analysis

Gene count values generated from fastq files in Star and M value matrices for mC and hmC were used in independent linear regression models (empirical bayes method) using the limma package (version 3.48.0) to identify differentially expressed genes and differentially methylated (DMP) and hydroxymethylated (DHP) positions in response to TCS, ICS and LPG compared to AA (Ritchie et al., 2015). Within subject correlation for matched samples (donor and occasion) across each exposure was included to ensure all identified changes were consistent across donors and reduce the impact of between donor differences. For RNA-seq data, log-CPM mean-variance relationship is accommodated using precision weights calculated by the voom function. For gene expression data, a linear model was performed for the discovery and replication experiments separately. Genes reaching Benjamini-Hochberg false discovery rate (FDR) < 0.05 in both analyses were taken forwards. For DNA methylation the replication experiment sample data were used and differentially methylated CpGs (DMPs) and differentially hydroxymethylated CpGs (DHPs) were considered significant at FDR <0.05.

2.6.2. Integration of gene expression and DNA methylation/hydroxymethylation

Association of methylation/hydroxymethylation changes with differential expression was studied using targeted analysis and expression quantitative trait methylation (eQTM) analysis. *Targeted Analysis*: CpG sites annotated to differentially expressed genes obtained from comparing TCS exposure to AA were identified by matching the gene names to the "UCSC_RefGene_Name" column in Illumina Human Methylation EPIC array annotation. Simple linear regression analysis was performed on DNA methylation/hydroxymethylation data at these CpGs to identify differential methylation between TCS and AA conditions. *eQTM:* The 52 consistently differentially expressed genes, and the 1303 DMPs and 3072 DHPs resulting from linear regression analysis to TCS smoke extract exposure, were used as the eQTM input to the limma package to identify significant gene-DMP/DHP pairs. eQTM pairs were considered significant at FDR <0.05.

2.6.3. Pathway analysis

Gene expression pathway analysis was carried out using IPA (QIAGEN Inc., https://www.qiagenbioinformatics.com/products/ingenuity pathway-analysis). Pathway analysis for differentially methylated CpG sites were carried out using the gometh function in missMethyl package (version 1.26.1) in R (Phipson et al., 2016). This method performs gene set enrichment analysis after correcting probe number bias and accounting for multiple gene associations with a single CpG (Maksimovic et al., 2021). For both methods a *p value* of <0.05 was taken as significant.

3. Results

3.1. TCS smoke extract induces gene expression changes in primary HBECs

To explore the impact of different cookstoves and fuel sources on gene expression in airway epithelial cells, we treated HBECs with TCS, ICS, LPG smoke extract and AA samples for 24 h and assessed genome wide gene expression. Of 15798 transcripts analysed, linear modelling identified 360 (Benjamini-Hochberg FDR p < 0.05) differentially expressed genes in response to TCS in the discovery experiment (Fig. 1a). No significantly differentially expressed genes were identified in response to ICS or LPG (Fig. S1a/b). 52 genes were consistently differentially expressed in response to TCS in a second independent replication experiment (Fig. 1a yellow points and Fig. 1b, Table S2, full replication data Fig. S2). All 52 genes displayed a consistent direction of expression change in both experiments (44 upregulated, 8 downregulated), but with some variation in magnitude (Fig. 1c). Specific assessment of the 52 genes altered by TCS exposure in the ICS and LPG smoke extract exposed samples identified non-significant, reduced magnitude but consistent direction of change for 49 genes in ICS stimulated cells, and 31 genes in both ICS and LPG smoke extract exposed cells (Fig. 1d). Differential expression of the 52 genes was significantly enriched in five canonical pathways ($p < 0.05$, $z < -1$or >1 Fig. 2a). Positive z-scores, indicating pathway activation, were seen for hepatic fibrosis (*FTH1, FTL, IKBKG, TFRC*), xenobiotic metabolism (*FTL, GCLC, MGST1, NQO1*), pentose phosphate (*G6PD, PGD, TALDO1, TKT*) and NRF-2 mediated oxidative stress response (*FTH1, FTL, GCLC, GCLM, GPX2, GSR, MGST1, NQO1, SQSTM1, TXNRD1*) pathways. A negative z score, indicative of pathway inhibition was observed for the ferroptosis signalling pathway (*AIFM2, FTH1, FTL, GCLC, SLC3A2, SLC7A11, SQSTM1, TFRC, TXNRD1*). Genes were predicted to be regulated by thirteen upstream regulators ($p < 0.05$, $z < -1$or >1 Fig. 2b) including NFE2L2, a transcription factor that regulates genes containing antioxidant response elements, and cytokines *IL-15* and *TNF*.

3.2. Smoke extracts induce distinct DNA methylation and hydroxymethylation changes in primary HBECs

Subsequently we studied changes in DNA methylation and hydroxymethylation to explore the potential underlying mechanism of gene expression regulation. Of 734,456 probes analysed, linear modelling identified 1303 (412 increased; 891 decreased), 6814 (3148 increased; 3666 decreased) and 6338 (2540 increased; 3798 decreased)

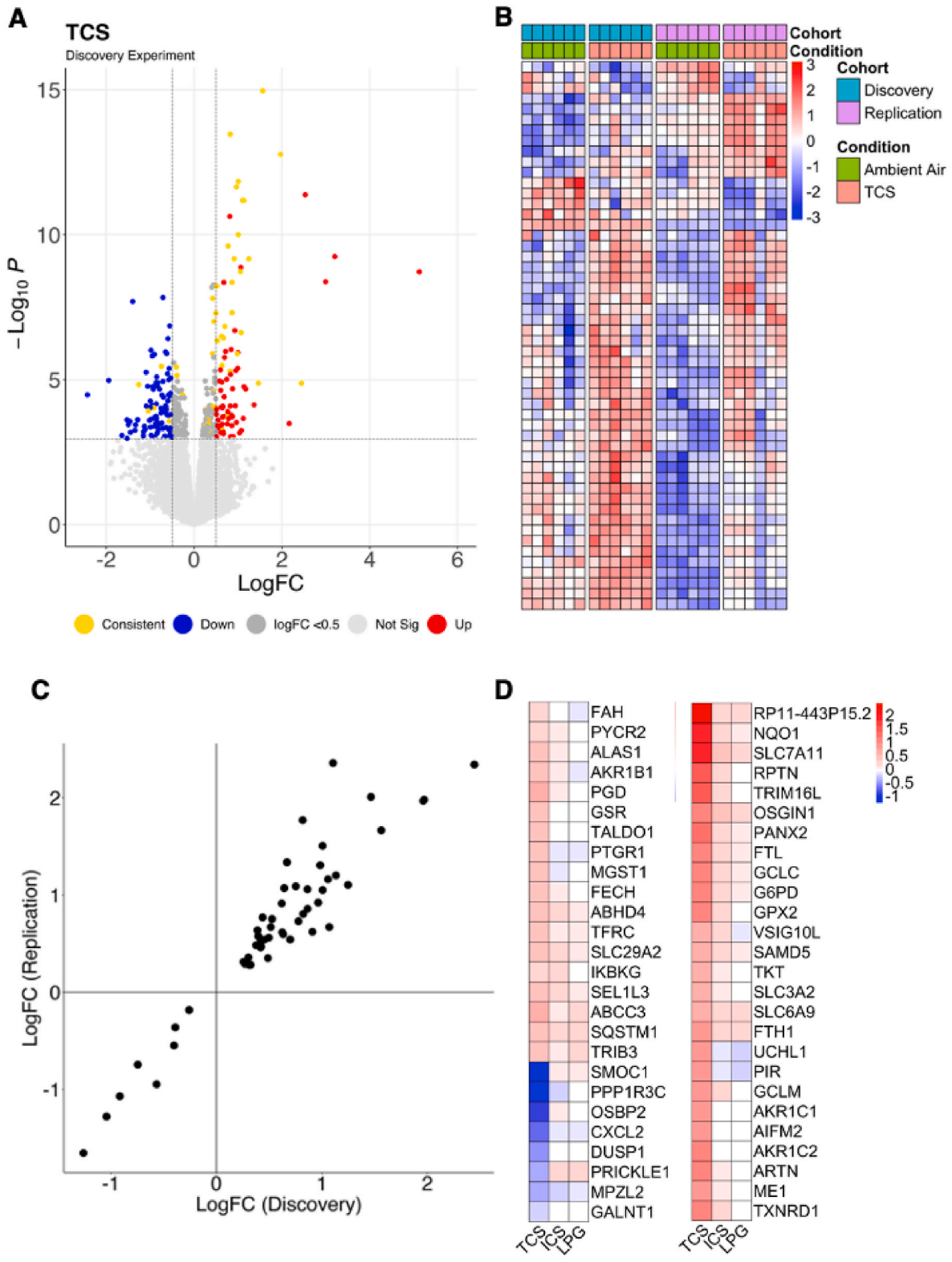

Fig. 1. Differential gene expression in HBECs exposed to TCS, ICS and LPG smoke extract. (A) *Plot of 15798 genes used in the analysis. red = upregulated, blue = downregulated, yellow =genes consistently altered in and replication.*(B) log-cpm of 52 consistently differentially expressed genes in ambient and TCS samples in all replicates in discovery and replication experiments. (C) Correlation of fold change in the 52 consistently differentially expressed genes in the discovery and replication experiments. (D) logFC of 52 consistent TCS induced genes in TCS, ICS and LPG relative to AA in discovery experiment.

significantly differentially methylated CpGs (DMPs) (Fig. 3a); and 3072 (1637 increased; 1435 decreased), 13536 (6961 increased; 6575 decreased) and 10662 (5568 increased; 5094 decreased) significantly differentially hydroxymethylated CpGs (DHPs) (Fig. 3b) in TCS, ICS and LPG smoke extract exposed HBECs respectively, compared to AA. Differentially methylated/hydroxymethylated sites were dispersed across all chromosomes with no enrichment to a particular genomic region (Fig. S3). Differential methylation and hydroxymethylation in

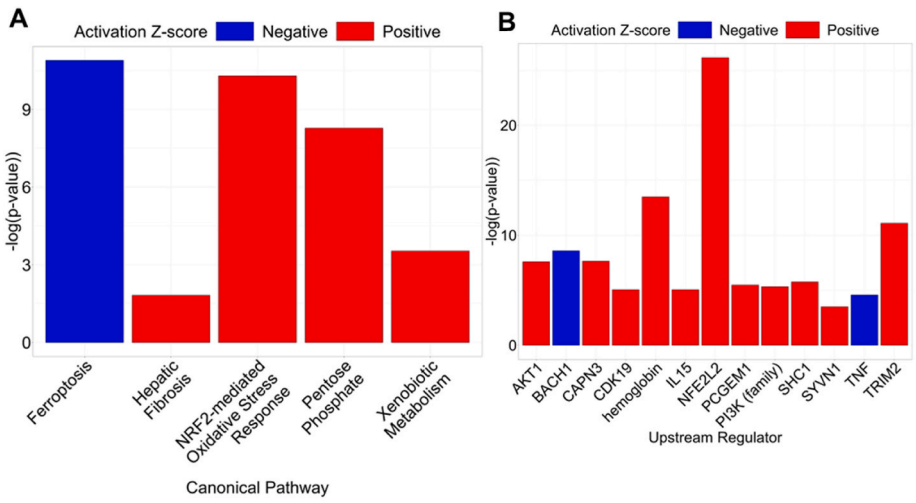

Fig. 2. Pathway analysis of 52 consistently differentially expressed genes. A) canonical pathways and B) upstream regulators enriched within TCS induced genes ($p < 0.05$ andz score >1 or < -1).

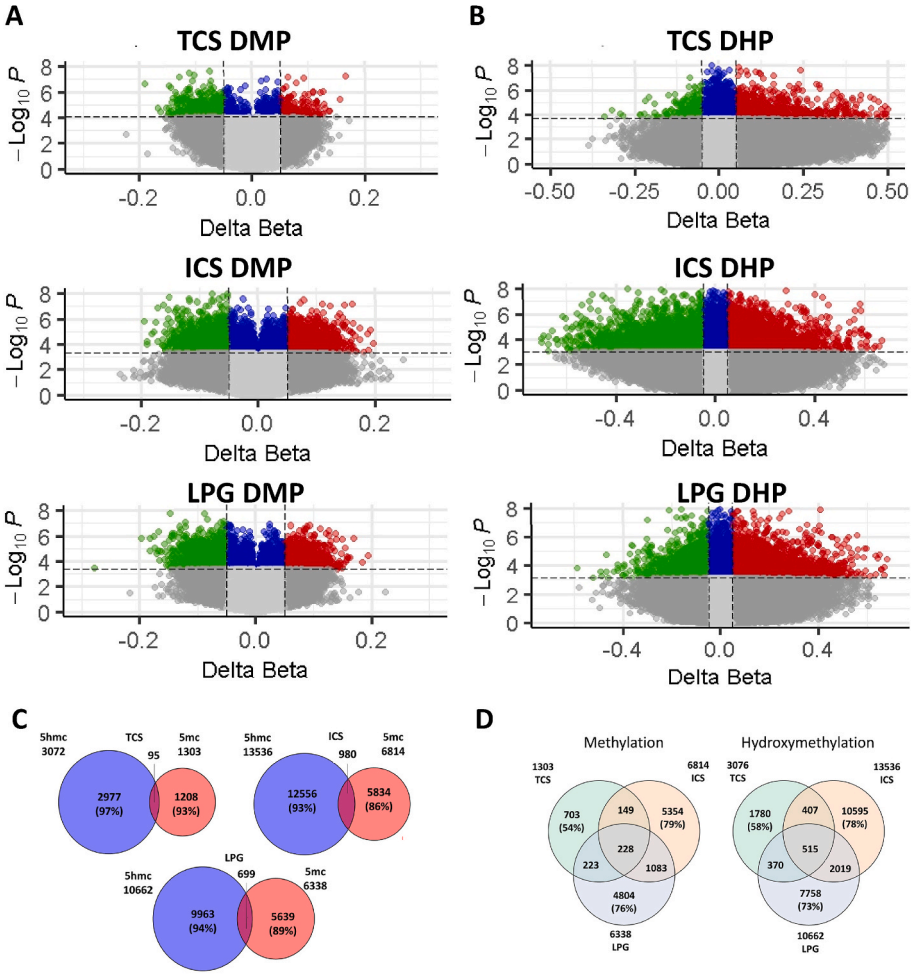

Fig. 3. Differential methylation (A) and hydroxymethylation (B) in HBECs exposed to cook stove smoke extracts. Plot of 734456 probes used in the analysis. Red = increased methylation/hydroxymethylation. Green decreased methylation/hydroxymethylation Horizontal dotted lines indicates p values corresponding to Benjamini-Hochberg FDR p 0.05. C) Overlap between mC and hmC in response to each cook stove smoke extract exposure. D) Overlap between the cook stove smoke extract exposure effect in comparison to ambient air within methylation and hydroxymethylation. Red font - Total number of DMPs and DHPs in each category.

response to the three smoke extracts were at primarily distinct CpG sites, with only 95, 980 and 699 of CpGs displaying both differential methylation and hydroxymethylation in response to TCS, ICS and LPG respectively (Fig. 3c), suggesting independent regulation of cytosine methylation and hydroxymethylation by cook stove smoke extract. Furthermore, there was limited overlap in CpG methylation or

hydroxymethylation between the three different cook stove smoke exposures, with only 228 DMPs and 515 DHPs co-identified across the three cookstove smoke extract exposed HBECs (Fig. 3d), suggesting distinct sites of cytosine modification modulation by the three different smoke extracts. As TCS and ICS both use biomass (of similar source) as the fuel, we identified overlap between TCS and ICS, independently of LPG. Thirty percent of TCS induced DMPs (377) and DHPs (922) overlapped with ICS induced counterparts (Fig. S4).

3.3. Differentially expressed genes in TCS exposed HBECs show association with mC and hmC changes

To understand if DNA methylation can mediate regulation of TCS induced gene expression we first used targeted analysis of CpGs annotated to the differentially expressed genes. 35 of the 52 TCS induced genes were annotated to 511 CpGs on the Illumina EPIC array (Table S3). 36 and 2 CpGs were differentially methylated and hydroxymethylated respectively between AA and TCS exposures and were annotated to 22 and 2 unique genes respectively (Table S3 and Fig. 4a). To understand any further association between DNA methylation/hydroxymethylation outside the formal Illumina array annotation, we performed eQTM using the 52 consistently differentially expressed genes, and the 1303 DMPs and 3072 DHPs resulting from linear regression analysis to TCS smoke extract exposure as the eQTM input. 100 significant methylation-gene expression pairs (MEP) (Figs. 4b) and 218 significant hydroxymethylation-gene expression pairs (HEP) were identified (Fig. 4c). The 100 MEPs consisted of fifteen unique genes and 88 unique CpGs while the 218 HEPs represented fourteen unique genes and 179 unique CpGs (Table 1). Fourteen genes (five upregulated and nine downregulated) were associated with both MEPs and HEPs, while a single gene (Malic Enzyme 1, ME1, upregulated) was associated with an MEP only. Ten of the 15 genes identified as MEP associated by eQTM were also genes identified as linked to differential DNA methylation via targeted analyses, despite different CpG associations (Table S3). Of the remaining 5 eQTM MEP associated genes, 4 did not have CpGs annotated to them on the array, while 15 CpGs annotated to SAMD5 were not identified as differentially methylated. The two genes for which targeted differentially hydroxymethylated CpGs were identified were not identified via eQTM analysis. The majority of eQTM expression linked CpGs were on distinct chromosomes to the associated gene (Fig. 4d). Only 6 MEP pairs (RPTN-cg03352242, AKR1C1-cg09311690, OSBP2-cg16186064, SLC7A11-cg18347227, SMOC1-cg18425804, PPP1R3C-cg25374057) (Fig. 4b, red points and Fig. 4d, red windows) and 5 HEP pairs (RPTN-cg21124756, AKR1C2-cg06948208, OSBP2-cg02226779, RP11-443P15.2-cg21919921, SAMD5) were present on the same chromosome (Fig. 4c, red points; Fig. 4d, red windows) with the distance between CpG and gene transcription start site always >500 kb, indicative of secondary signalling or complex chromatin configurations.

3.4. Underlying CpG modification is associated with specific functional aspects of gene expression

Subsequently, we were interested in understanding the potential functional effects of underlying CpG cytosine modifications on gene expression. At the pathway level, one methylation associated gene (eQTM and targeted), SLC7A11, was present in all five identified significant canonical gene expression pathways. SLC7A11 is a cell membrane bound cysteine/glutamate transporter at the start of the ferroptosis pathway (Fig. S5, Yellow highlight), the pathway most significantly associated with TCS exposure. Furthermore, targeted analysis identified DNA methylation associated genes were present in all thirteen identified upstream regulatory pathways, while eQTM identified DNA methylation associated genes were present in seven of the thirteen identified upstream regulatory pathways. This included nine genes identified by targeted analysis (*ABCC3, GSR, GCLM, ME1, TALDO1, PGD, SLC7A11, AKR1C1, AKR1C2*), and five genes identified by eQTM (*SLC7A11, AKR1C1, AKR1C2, ME1* and *ABCC3*) predicted to be regulated by NFE2L2. NFE2L2 is a downstream component of the ferroptosis pathway, and SLC7A11 is regulated by NFE2L2, potentially suggesting a DNA methylation mediated SLC7A11:NFE2L2 signalling feedback loop (Fig. S6). Furthermore, if the ferroptosis and NFE2L2 pathways are considered in combination all 14 eQTM associated genes (Fig. S6 blue bold text) and 20/22 targeted methylation associated genes (Fig. S6, red asterisks) can be linked via a tumorigenesis intermediate, identifying DNA methylation as a potential key intermediate in downstream cellular effects of TCS exposure.

3.5. Non-gene expression associated alterations to DNA (hydroxy) methylation are linked to distinct biological processes and molecular pathways

Finally, we aimed to understand the potential function of alterations to DNA methylation and hydroxymethylation not concurrently associated with changes in gene expression. In line with the minimal overlap between exposure associated differentially methylated and hydroxymethylated CpGs, pathway analysis of DMPs and DHPs identified different enriched pathways for all three smoke extract types, and for CpG methylation versus hydroxymethylation (Fig. S7; A) Biological Processes, B) Molecular functions). TCS methylcytosine modification was enriched for neutrophil apoptotic/regulation biological pathways, a processimplicated in airway response to diesel exhaust exposure (Shin et al., 2022), and phosphatidylinositol bisphosphate kinase activity molecular function, known to mediate neutrophil function (Luo et al., 2015). TCS hydroxymethylcytosine biological process enrichment was more diverse but associated with molecular functions enriched consistently for transforming growth factor beta (TGFβ) receptor activation, a signalling pathway implicated in epithelial-mesenchymal transition in response to particulate matter exposure (Xu et al., 2019). ICS smoke extract exposure enriched for CpGs annotated to genes involved in small GTPase/Ras signal transduction/activation in both biological processes and molecular functions, pathways potentially activated by exposure induced reactive nitrogen/oxygen species (Davis et al., 2011). Finally, LPG associated differential methylation linked to platelet derived growth factor (PDGF) signalling biological processes, protein phosphatase activity and GTPase activity molecular functions. PDGF receptor expression is upregulated in lung fibroblasts in response to particulate matter with an aerodynamic diameter of <10 μm (PM_{10}) (Xu et al., 2019; Bonner et al., 1998). While LPG associated hydroxymethyl changes were associated with cell junction organisation and focal adhesion assembly biological processes and actin/cytoskeletal protein molecular processes, implicating a link to cell adhesion and barrier formation (Smyth et al., 2020; Doornaert et al., 2003). A single biological process, cell junction organisation, was in common across all hydroxymethyl associations regardless of cook stove type suggesting a stronger role for hydroxymethylcytosine methylation in this process.

4. Discussion

Here we report that acute exposure of human airway epithelial cells *in vitro* for 24 h to smoke extracts collected from traditional, improved and LPG cook stoves in Nepal induce distinct gene expression, DNA methylation and DNA hydroxymethylation changes. Significant gene expression changes were only observed in response to TCS smoke extract, although smaller, non-significant changes were seen for many of the same genes with ICS extract. TCS smoke extract induced gene expression enriched to ferroptosis and NRF2-oxidative stress pathways and to the upstream regulator NFE2L2. Significant DNA methylation and hydroxymethylation changes were observed in response to all three smoke extracts, with primarily distinct alterations to each exposure type. Fourteen and 22 of the 52 consistently (across discovery and replication) differentially expressed genes were associated with DNA

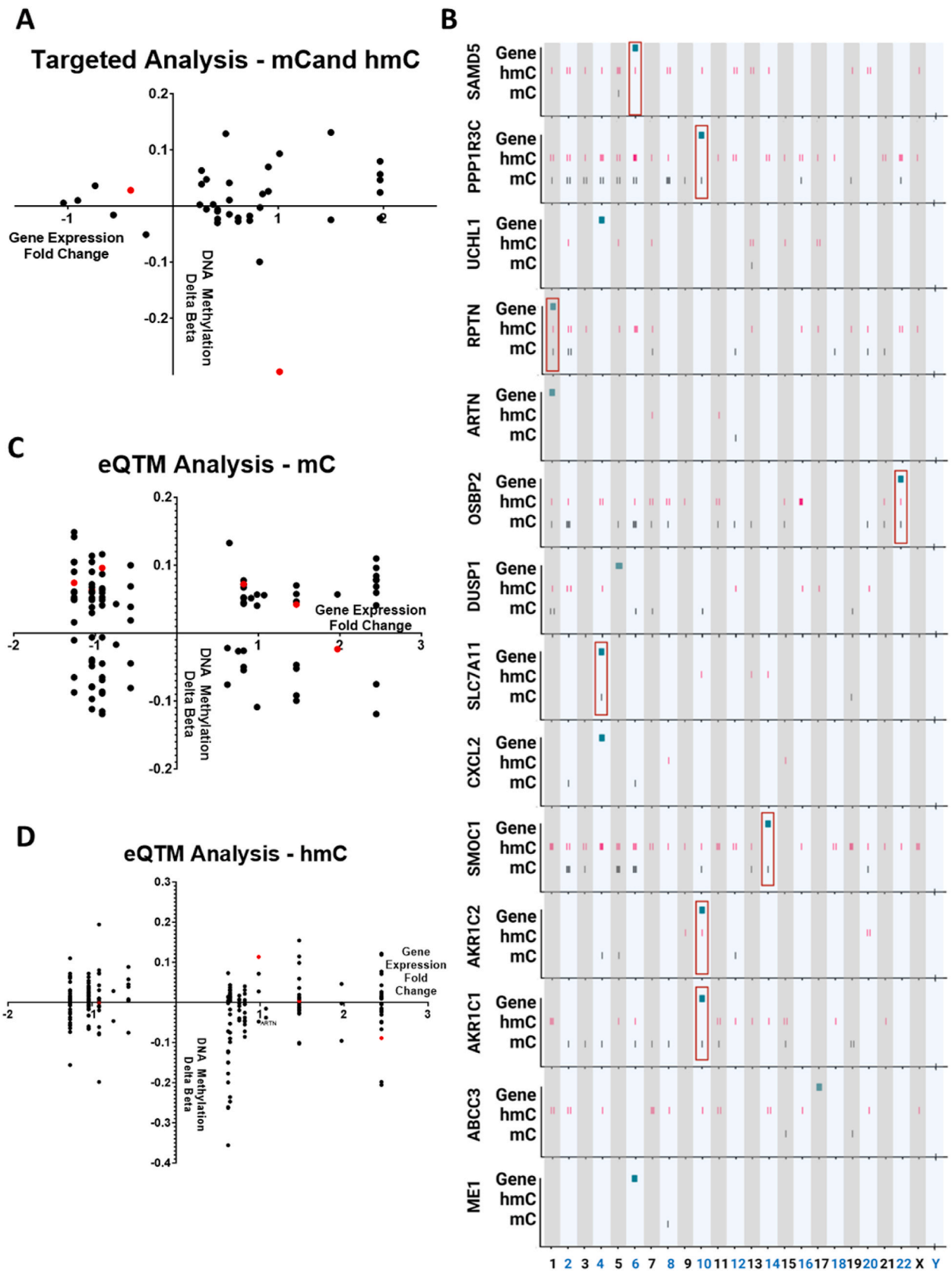

Fig. 4. Association of gene expression and DNA methylation/hydroxymethylation. A) Correlation plot of the 36 gene-cpg pairs from targeted analysis Black points = methyl cytosine associated, red points = hydroxymethylcytosine associated. B) Correlation plot of the 100 MEPs from eQTM analysis. Red = Cis MEP pairs C) Correlation plot of the 218 HEPs from eQTM analysis. Red = Cis HEP pairs D) Distribution of differential gene expression associated methylation/hydroxymethylation sites across the chromosomes. Red windows = Cis associations.

Table 1
Differentially expressed genes with DNA methylation and hydroxymethylation changes.

Associated Genes	Gene Name	Number of Associated CpGs	
		Methylation	Hydromethylation
SMOC1	SPARC related modular calcium binding 1	15	43
RP11-443P15.2	RP11-443P15.2 (Clone-based (Vega) gene)	10	24
AKR1C1	Aldo-keto reductase family 1 member C1	11	14
PPP1R3C	Protein phosphatase 1 regulatory subunit 3C	20	32
DUSP1	Dual specificity phosphatase 10	6	8
OSBP2	Oxysterol binding protein 2	17	20
SAMD5	Sterile alpha motif domain containing 5	1	21
CXCL2	C-X-C motif chemokine ligand 2	2	2
RPTN	Repetin	8	20
ABCC3	ATP binding cassette subfamily C member 3	2	17
AKR1C2	Aldo-keto reductase family 1 member C2	3	4
SLC7A11	Solute carrier family 7 member 11	2	3
UCHL1	Ubiquitin C-terminal hydrolase L1	1	8
ARTN	Artemin	1	2
ME1	Malic enzyme 1	1	0

methylation and hydroxymethylation changes by eQTM and targeted analysis respectively, including key genes within the ferroptosis and NFE2L2 pathways, both relevant to airway biology and lung disease. These data identify differential effects of cookstove smoke extracts on airway epithelial cell gene expression and DNA cytosine modifications. The highlighted pathways and regulators are important in lung biology and provide further evidence for the effects of indoor air pollution on lung disease.

Ferroptosis is a necrotic form of regulated cell death, dependent on iron and phospholipid peroxidation of plasma membranes by reactive oxygen species (Dixon et al., 2012). Cigarette smoke extract induces ferroptosis in human airway epithelial cells (Yoshida et al., 2019) and bronchoalveolar epithelial cells (Lian et al., 2021) and ferroptosis plays a role in cigarette smoke-induced pathogenesis of chronic obstructive pulmonary disease (COPD) in mice (Yoshida et al., 2019). Stimulation of ferroptosis induces pro-inflammatory cytokine release from epithelial cells, leading to an inflammatory cascade previously implicated in COPD-related airway remodelling and emphysema (Lian et al., 2021). The NF-E2-realted 2 (Nrf2) transcription factor binds to antioxidant response elements in DNA to regulate transcriptional events that protect respiratory cells against reactive oxygen species induced by toxins and inflammation (Jennifer Carlson, 2020). *In vitro*, exposure of nasal cell line RPMI 2650 to $PM_{2.5}$ induces Nrf2 nuclear translocation (Hong et al., 2016) and diesel exhaust particle induction of ARE-mediated gene expression is dependent on Nrf2 in murine macrophages (Yoshida et al., 2019; Li et al., 2004) and bronchoalveolar epithelial cells (Lian et al., 2021) suggestive of a general responsiveness of Nrf2 to air pollutants. Nrf2 levels are associated with asthma severity (Youness et al., 2020) and, in mice, Nrf2 knockout worsens response to allergen challenge and reduces stretch/increases airways resistance in response to methacholine (Rangasamy et al., 2005). Furthermore, in an elastase mouse models of COPD, Nrf2 knock down exacerbates elastase induced alveolar wall damage and airspace enlargement (Ishii et al., 2005), while the single nucleotide polymorphism rs35652124 present within the *NFE2L2* gene is associated with COPD risk in smoking individuals (Korytina et al., 2019). The true prevalence of airways disease and formal disease diagnosis in rural Nepalese populations using these cooking stoves are difficult to determine. This data provide evidence that exposure of the airway epithelium to traditional cookstove smoke activates pathways and regulators associated with asthma and Chronic Obstructive Pulmonary Disease (COPD) that a transition to "cleaner" technologies could prevent.

Although significant gene expression changes were only observed in response to TCS smoke extract exposure, smaller (non-significant) changes in expression of 49 of the 52 genes (all except *AIFM2, PRICKLE1 and PTGR1*) were observed in a consistent direction of change in response to ICS smoke exposure. This is likely due to use of the same type of fuel source under effectively diluted conditions due to improved smoke extraction systems when using ICS. We have previously shown that in households using ICS, the mean exposure to $PM_{2.5}$ is reduced by 51% and carbon monoxide concentrations are 72% lower (Kc et al., 2020). Interestingly, 31 of the TCS gene changes were also altered in a consistent direction but reduced magnitude and significance in response to LPG, suggesting factors other than fuel source may drive this subset of genes. Smoke extracts are complex solutions but our approach to bubble smoke through media to collect both particulate and soluble/volatile components was designed to mimic as closely as possible true exposure of the lung. Constituent analysis of the exposures in future studies would facilitate detailed elucidation of differential exposure effects.

In contrast to gene expression, primarily distinct DNA methylation and hydroxymethylation changes were observed in response to all three smoke extract exposures, primarily in isolation to gene expression changes. These data are limited by the lack of replication data and the functional impact of non-gene associated changes in DNA methylation and hydroxymethylation remain to be fully determined, however pathway analysis identified distinct associations for methylation and hydroxymethylation changes in response to each exposure. While pathway analysis on DNA methylation changes should be treated with caution due to limitations in how CpGs are linked to annotated genes, the pathways identified were relevant to airway biology and disease, including neutrophil function, TGFβ/PDGF signalling and barrier formation. They were also consistent with previous reports of biomass exposure effects on DNA methylation changes at genes annotated to GTPase activity and growth factor signalling pathways in airway epithelial cell line BEAS-2B (Hesselbach et al., 2017). Similar to gene expression those sites that were specific to TCS exposure did display the same direction of change in response to TCS and ICS exposure but with variations in magnitude. We also saw minimal overlap between exposure induced changes in DNA methylation and hydroxymethylation, suggesting exposures mediate these two DNA modifications independently as reported previously in airway epithelial cells exposed to diesel exhaust particles (Zhang et al., 2018). However, we were unable to undertake a formal comparison without publicly available data. Hydroxymethylcytosine can be enriched without DNA demethylation, implicating hydroxymethylcytosine as a stable epigenetic mark in its own right (Hahn et al., 2013), and further study of this in response to inhaled exposures is warranted.

We observed a predominance of decreased CpG methylcytosine in response to all cookstove smoke exposures which is common in epithelial cell responses to air pollutants (Clifford, 2017; Hesselbach et al., 2017; Zhang et al., 2018; Bind et al., 2014). Our hydroxymethylcytosine data showed a slight predominance to increased hydroxymethylation, in agreement with increases in global blood DNA hydroxymethylation in association with particulate matter concentrations in truck drivers and office workers in Beijing (Sanchez-Guerra et al., 2015), and site specific hydroxymethylation in human airway epithelial cells exposed to diesel exhaust particles (Zhang et al., 2018). However, ours in only the second study of site specific hydroxymethylcytosine response to an air pollutant and further studies that distinguish methyl and hydroxymethyl responses to comparative inhaled exposures are required. Furthermore, the methodology for processing and analysing hydroxymethyl data are less developed than

for methylcytosine. In particular, the methods to distinguish methylcytosine from hydroxymethylation, and the statistical analysis of the two resulting datasets with very different distributions. We selected a maximum likelihood methylation levels (MLML) method for methylcytosine versus hydroxymethylcytosine identification, as it does not suffer from the generation of negative hydroxymethylcytosine values and sums of unmodified, methylcytosine and hydroxymethylcytosine totalling greater than one due to technical error seen in subtraction methods (Kiihl et al., 2019b). For differential hydroxymethylation analysis we selected linear modelling as we had used for methylcytosine and has been used by others for hydroxymethylcytosine analysis (Solomon et al., 2019; Skvortsova et al., 2017; Spiers et al., 2017). We did validate a selection of targets by non-parametric Mann-Whitney analysis (Fig. S8) but raise awareness of inherent differences in hydroxymethylation data that may alter its handling to methylcytosine data.

The current study has some limitations. Whilst replication experiments were available for gene expression studies a separate replication study was not available for the DNA methylation data. However, we have previously validated array DNA methylation difference and observed high technical correlation between beta values generated by the array and by pyrosequencing (Clifford et al., 2018; Clifford et al., 2020; Clifford et al., 2019), and have high confidence in the technical accuracy of the platform. Secondly, the experiments conducted within each phase (termed discovery and replication) were performed in two donors (2 donors for discovery, 2 distinct donors for replication). However, experiments within each donor were repeated on three separate occasions (total of six samples per experiment) and analysis was performed within donor:repeat pair to ensure all findings reported are consistent regardless of biological and technical variability. Furthermore, while these experiments were undertaken in primary human epithelial cells, an improvement in biological relevance to exposure studies in immortalised epithelial cells (Hesselbach et al., 2017), we used submerged culture conditions which do not recapitulate the complexity of the airway epithelial barrier. Further study of responses in epithelium differentiated at air-liquid interface (ALI) would be a useful next step, especially given previous evidence of differential responses of submerged versus ALI cultures to ambient air pollution exposure (Ghio et al., 2013). Cell cycle arrest has been reported in response to air pollutants, for example $PM_{2.5}$ from Shenyang, China (Zhang et al., 2019) and atmospheric residential urban PM_{10} (Reyes-Zarate et al., 2016) but was not assessed here and would be interesting to understand in response to these specific exposures in future work. We assessed gene expression and DNA methylation changes at a single time point, preventing an assessment of the longevity of the responses. A preliminary analysis of a chronic exposure study identified differential expression of 13 of the 52 differentially TCS exposed expressed genes were maintained under chronic exposure (Fig. S9), four of which we identified as associated with alterations to DNA methylation. This indicates a proportion of genes may maintain altered expression in response to continued exposure, and DNA methylation may in part mediate those changes. Finally, we used a short-term exposure model to study immediate epithelial cell responses to exposure however a chronic model would provide further information on the effects of long term, repeated exposures as occurs in real life cooking environments.

5. Conclusion

Our study demonstrates short-term exposure to cookstove smoke extracts induces acute alterations to gene expression, DNA methylation and hydroxymethylation. Significant gene expression changes were restricted to TCS exposure, although similar trends were observed for the same genes with ICS exposure. All three exposures associated with changes in both DNA methylation and hydroxymethylation. Gene expression and DNA methylation and hydroxymethylation were linked in a subset of genes in response to TCS exposure, enriching for the ferroptosis pathway and NFE2L2 regulation, implicating DNA cytosine modification as a molecular mechanism involved in expression regulation of these pathways. DNA methylation and hydroxymethylation changes without association to a concurrent change in gene expression were linked to pathways relevant to airway biology and warrant further study of their functional impact, as does the long-term impact of DNA methylation changes. The responses we have identified are likely to drive altered airway responses in vivo and may contribute to development of respiratory disease. Reducing exposure, for example with use of improved cook stoves, reduces gene expression changes and is therefore likely to be beneficial to health. Overall, these data provide further insights into the observed association between indoor air pollution exposure and chronic lung disease.

Author contributions

Poojitha Rajasekar: Methodology, software, Formal analysis, writing -original draft, visualization, Robert Hall: Methodology, software, Formal analysis, writing -original draft, visualization, Binaya KC: Conceptualization, methodology, resources, Writing - Review & Editing, Parth S. Mahapatra: Resources, Writing - Review & Editing, Siva P. Puppala: Resources, Writing - Review & Editing, Dhruma Thakker: Investigation, Writing - Review & Editing, Julia L MacIsaac: Investigation, Resources, Writing - Review & Editing, David Lin: Investigation, Resources, Writing - Review & Editing, Michael Kobor: Resources, Writing - Review & Editing, Charlotte E Bolton: Conceptualization, Writing - Review & Editing, Supervision, funding acquisition, Ian Sayers: Conceptualization, Methodology, Writing - Review & Editing, Supervision, Ian P. Hall: Conceptualization, Writing - Review & Editing, Supervision, project administration, funding acquisition, Rachel L. Clifford: Conceptualization, Methodology, Writing -original draft, Writing - Review & Editing, Supervision. All authors approved the final version for submission.

Financial Support

This work was supported by Global Challenges Research Fund Interdisciplinary Research Project “Improving Respiratory Health in Nepal” (Research England) awarded to the University of Nottingham. This research was supported in part by the NIHR Nottingham Biomedical Research Centre (PR, RH, DT, CEB, IS, IPH, RC). IPH holds an NIHR Senior Investigator Award. RC is supported by a University of Nottingham Anne McLaren Fellowship. Funders had no role in the study design, collection, analysis/interpretation of data, writing of the report or decision to submit for publication.

Declaration of competing interest

The authors declare the following financial interests/personal relationships which may be considered as potential competing interests: Poojitha Rajasekar reports travel was provided by Asthma and Lung UK. Ian Hall and Charlotte Bolton reports financial support was provided by Global Challenges Research Fund. Ian Sayers and Ian Hall reports financial support was provided by NIHR Nottingham Biomedical Research Centre. Rachel Clifford reports financial support was provided by University of Nottingham. Ian Hall and Ian Sayers reports a relationship with GSK, BBSRC, Wellcome Trust, Boeringer Ingelheim that includes: board membership, funding grants, and speaking and lecture fees. Ian Hall is Vice Chair Trustees for Asthma + Lung UK and Chair of the Swedish Research Council ALF3 panel. All other authors have nothing to disclose.

Data availability

Data will be made publicly available upon publishing

Appendix A. Supplementary data

Supplementary data to this article can be found online at https://doi.org/10.1016/j.envpol.2023.122561.

References

Andrews, S., FastQC: a quality control tool for high throughput sequence data *[Online]. Available online at:* http://www.bioinformatics.babraham.ac.uk/projects/fastqc/.2010..

Aryee, M.J., et al., 2014. Minfi: a flexible and comprehensive Bioconductor package for the analysis of Infinium DNA methylation microarrays. Bioinformatics 30 (10), 1363–1369.

Audrey Lejart, G.S., 2018. Sébastien Huet *Cytosine hydroxymethylation by TET enzymes: From the control of gene expression to the regulation of DNA repair mechanisms, and back*. AIMS Biophysics 5 (3), 182–193.

Bind, M.A., et al., 2014. Air pollution and gene-specific methylation in the Normative Aging Study: association, effect modification, and mediation analysis. Epigenetics 9 (3), 448–458.

Bolger, A.M., Lohse, M., Usadel, B., 2014. Trimmomatic: a flexible trimmer for Illumina sequence data. Bioinformatics 30 (15), 2114–2120.

Bonner, J.C., et al., 1998. Induction of the lung myofibroblast PDGF receptor system by urban ambient particles from Mexico City. Am. J. Respir. Cell Mol. Biol. 19 (4), 672–680.

Cao, Y., et al., 2020. Environmental pollutants damage airway epithelial cell cilia: implications for the prevention of obstructive lung diseases. Thorac Cancer 11 (3), 505–510.

Chi, G.C., et al., 2016. Long-term outdoor air pollution and DNA methylation in circulating monocytes: results from the Multi-Ethnic Study of Atherosclerosis (MESA). Environ. Health 15 (1), 119.

Clifford, R.L., et al., 2017. Inhalation of diesel exhaust and allergen alters human bronchial epithelium DNA methylation. J. Allergy Clin. Immunol. 139 (1), 112–121.

Clifford, R.L., et al., 2018. Altered DNA Methylation Is Associated with Aberrant Gene Expression in Parenchymal but Not Airway Fibroblasts Isolated from Individuals with COPD. Clinical Epigenetics, p. 10.

Clifford, R.L., et al., 2019. Airway epithelial cell isolation techniques affect DNA methylation profiles with consequences for analysis of asthma related perturbations to DNA methylation. Sci. Rep. 9.

Clifford, R.L., et al., 2020. TWIST1 DNA methylation is a cell marker of airway and parenchymal lung fibroblasts that are differentially methylated in asthma. Clin. Epigenet. 12 (1).

Davis, M.F., Vigil, D., Campbell, S.L., 2011. Regulation of Ras proteins by reactive nitrogen species. Free Radic. Biol. Med. 51 (3), 565–575.

Dixon, S.J., et al., 2012. Ferroptosis: an iron-dependent form of nonapoptotic cell death. Cell 149 (5), 1060–1072.

Dobin, A., et al., 2013. STAR: ultrafast universal RNA-seq aligner. Bioinformatics 29 (1), 15–21.

Doornaert, B., et al., 2003. Negative impact of DEP exposure on human airway epithelial cell adhesion, stiffness, and repair. Am. J. Physiol. Lung Cell Mol. Physiol. 284 (1), L119–L132.

Fortin, J.P., Triche, T.J., Hansen, K.D., 2017. Preprocessing, normalization and integration of the Illumina HumanMethylationEPIC array with minfi. Bioinformatics 33 (4), 558–560.

Fujii, T., et al., 2001. Particulate matter induces cytokine expression in human bronchial epithelial cells. Am. J. Respir. Cell Mol. Biol. 25 (3), 265–271.

Ghio, A.J., et al., 2013. Growth of human bronchial epithelial cells at an air-liquid interface alters the response to particle exposure. Part. Fibre Toxicol. 10, 25.

Hahn, M.A., et al., 2013. Dynamics of 5-hydroxymethylcytosine and chromatin marks in Mammalian neurogenesis. Cell Rep. 3 (2), 291–300.

Hall, R.J., et al., 2021. Functional genomics of GPR126 in airway smooth muscle and bronchial epithelial cells. Faseb. J. 35 (7), e21300.

Hesselbach, K., et al., 2017. Disease relevant modifications of the methylome and transcriptome by particulate matter (PM2.5) from biomass combustion. Epigenetics 12 (9), 779–792.

Hong, Z., et al., 2016. Airborne fine particulate matter induces oxidative stress and inflammation in human nasal epithelial cells. Tohoku J. Exp. Med. 239 (2), 117–125.

Ishii, Y., et al., 2005. Transcription factor Nrf2 plays a pivotal role in protection against elastase-induced pulmonary inflammation and emphysema. J. Immunol. 175 (10), 6968–6975.

Jennifer Carlson, L.P., 2020. Huai Dengcorresponding author, Nrf2 and the Nrf2-interacting Network in respiratory inflammation and diseases. Nrf2 and its Modulation in Inflammation 85, 51–76.

Jiang, X.Q., Mei, X.D., Feng, D., 2016. Air pollution and chronic airway diseases: what should people know and do? J. Thorac. Dis. 8 (1), E31–E40.

Jiang, Y., et al., 2022. Human airway organoids as 3D in vitro models for a toxicity assessment of emerging inhaled pollutants: tire wear particles. Front. Bioeng. Biotechnol. 10, 1105710.

Kc, B., et al., 2020. Proinflammatory effects in Ex vivo human lung tissue of respirable smoke extracts from indoor cooking in Nepal. Ann Am Thorac Soc 17 (6), 688–698.

Kiihl, S.F., et al., 2019a. MLML2R: an R package for maximum likelihood estimation of DNA methylation and hydroxymethylation proportions. Stat. Appl. Genet. Mol. Biol. 18 (1).

Kiihl, S.F., et al., 2019b. MLML2R: an R package for maximum likelihood estimation of DNA methylation and hydroxymethylation proportions. Stat. Appl. Genet. Mol. Biol. 18 (1).

Korytina, G.F., et al., 2019. Associations of the NRF2/KEAP1 pathway and antioxidant defense gene polymorphisms with chronic obstructive pulmonary disease. Gene 692, 102–112.

Leek, J.T., et al., 2012. The sva package for removing batch effects and other unwanted variation in high-throughput experiments. Bioinformatics 28 (6), 882–883.

Li, N., et al., 2004. Nrf2 is a key transcription factor that regulates antioxidant defense in macrophages and epithelial cells: protecting against the proinflammatory and oxidizing effects of diesel exhaust chemicals. J. Immunol. 173 (5), 3467–3481.

Li, H., et al., 2021. Predominant DNMT and TET mediate effects of allergen on the human bronchial epithelium in a controlled air pollution exposure study. J. Allergy Clin. Immunol. 147 (5), 1671–1682.

Lian, N., et al., 2021. The role of ferroptosis in bronchoalveolar epithelial cell injury induced by cigarette smoke extract. Front. Physiol. 12, 751206.

Luo, H.R., Mondal, S., 2015. Molecular control of PtdIns(3,4,5)P3 signaling in neutrophils. EMBO Rep. 16 (2), 149–163.

Maksimovic, J., Oshlack, A., Phipson, B., 2021. Gene set enrichment analysis for genome-wide DNA methylation data. Genome Biol. 22 (1), 173.

Montgomery, M.T., et al., 2020. Genome-wide analysis reveals Mucociliary remodeling of the nasal airway epithelium induced by urban PM2.5. Am. J. Respir. Cell Mol. Biol. 63 (2), 172–184.

Organisation, W.H., 2021. Household air pollution and health [cited 2021 23rd November]; Available from: https://www.who.int/news-room/fact-sheets/detail/household-air-pollution-and-health.

Panni, T., et al., 2016. Genome-wide analysis of DNA methylation and fine particulate matter air pollution in three study populations: KORA F3, KORA F4, and the Normative aging study. Environ. Health Perspect. 124 (7), 983–990.

Paudel, D., Jeuland, M., Lohani, S.P., 2020. Cooking-energy transition in Nepal: trend review. Clean Energy 5 (1), 1–9.

Phipson, B., Maksimovic, J., Oshlack, A., 2016. missMethyl: an R package for analyzing data from Illumina's HumanMethylation450 platform. Bioinformatics 32 (2), 286–288.

Pidsley, R., et al., 2013. A data-driven approach to preprocessing Illumina 450K methylation array data. BMC Genom. 14 (1), 293.

Pidsley, R., et al., 2016. Critical evaluation of the Illumina MethylationEPIC BeadChip microarray for whole-genome DNA methylation profiling. Genome Biol. 17.

Qu, J., et al., 2013. MLML: consistent simultaneous estimates of DNA methylation and hydroxymethylation. Bioinformatics 29 (20), 2645–2646.

Raju, S., Siddharthan, T., McCormack, M.C., 2020. Indoor air pollution and respiratory health. Clin. Chest Med. 41 (4), 825–843.

Rangasamy, T., et al., 2005. Disruption of Nrf2 enhances susceptibility to severe airway inflammation and asthma in mice. J. Exp. Med. 202 (1), 47–59.

Rayner, R.E., et al., 2019. Optimization of normal human bronchial epithelial (NHBE) cell 3D cultures for in vitro lung model studies. Sci. Rep. 9 (1), 500.

R.C.T. and R 2020), R.C.T., R : A language and environment for statistical computing. R Foundation for Statistical Computing , Vienna, Austria.

Reyes-Zarate, E., et al., 2016. Atmospheric particulate matter (PM10) exposure-induced cell cycle arrest and apoptosis evasion through STAT3 activation via PKC zeta and Src kinases in lung cells. Environ. Pollut. 214, 646–656.

Ritchie, M.E., et al., 2015. Limma powers differential expression analyses for RNA-sequencing and microarray studies. Nucleic Acids Res. 43 (7).

Robinson, M.D., McCarthy, D.J., Smyth, G.K., 2010. edgeR: a Bioconductor package for differential expression analysis of digital gene expression data. Bioinformatics 26 (1), 139–140.

Sanchez-Guerra, M., et al., 2015. Effects of particulate matter exposure on blood 5-hydroxymethylation: results from the Beijing truck driver air pollution study. Epigenetics 10 (7), 633–642.

Shi, Y., et al., 2019. PM2.5-induced alteration of DNA methylation and RNA-transcription are associated with inflammatory response and lung injury. Sci. Total Environ. 650 (Pt 1), 908–921.

Shin, J.W., et al., 2022. A unique population of neutrophils generated by air pollutant-induced lung damage exacerbates airway inflammation. J. Allergy Clin. Immunol. 149 (4), 1253–1269 e8.

Skvortsova, K., et al., 2017. Comprehensive Evaluation of Genome-wide 5-hydroxymethylcytosine Profiling Approaches in Human DNA, vol. 10. Epigenetics & Chromatin.

Smyth, T., et al., 2020. Diesel exhaust particle exposure reduces expression of the epithelial tight junction protein Tricellulin. Part. Fibre Toxicol. 17 (1), 52.

Solomon, O., et al., 2019. 5-Hydroxymethylcytosine in cord blood and associations of DNA methylation with sex in newborns. Mutagenesis 34 (4), 315–322.

Spiers, H., et al., 2017. 5-hydroxymethylcytosine is highly dynamic across human fetal brain development. BMC Genom. 18.

Wang, C., et al., 2020. Long-term ambient fine particulate matter and DNA methylation in inflammation pathways: results from the Sister Study. Epigenetics 15 (5), 524–535.

Xu, Z., Ding, W., Deng, X., 2019. PM2.5, fine particulate matter: a Novel player in the epithelial-mesenchymal transition? Front. Physiol. 10, 1404.

Yoshida, M., et al., 2019. Involvement of cigarette smoke-induced epithelial cell ferroptosis in COPD pathogenesis. Nat. Commun. 10 (1), 3145.

Youness, E.R., et al., 2020. The role of serum nuclear factor erythroid 2-related factor 2 in childhood bronchial asthma. J. Asthma 57 (4), 347–352.
Zhang, X., et al., 2018. Diesel exhaust and house dust mite allergen lead to common changes in the airway methylome and hydroxymethylome. Environ Epigenet 4 (3), dvy020.
Zhang, Y., et al., 2019. PM2.5 induces cell cycle arrest through regulating mTOR/P70S6K1 signaling pathway. Exp. Ther. Med. 17 (6), 4371–4378.